# Magma vesiculation and infrasonic activity at Stromboli open conduit vocano

Earth and Planetary Science Letters 292 (2010) 274–280

Contents lists available at ScienceDirect

Earth and Planetary Science Letters

journal homepage: www.elsevier.com/locate/epsl

# Magma vesiculation and infrasonic activity at Stromboli open conduit volcano

Livia Colò [a], Maurizio Ripepe [a,*], Don R. Baker [b], Margherita Polacci [c]

[a] Università degli Sudi di Firenze, Dipartimento di Scienze della Terra, via la Pira 4, 50121, Firenze, Italy
[b] Earth and Planetary Sciences, McGill University, 3450 rue University, Montreal, QC, Canada H3A 2A7
[c] Istituto Nazionale di Geofisica e Vulcanologia, sezione di Pisa, via della Faggiola 32, 56126, Pisa, Italy

ARTICLE INFO

*Article history:*
Received 10 April 2009
Received in revised form 20 October 2009
Accepted 8 January 2010
Available online 2 March 2010

Editor: L. Stixrude

*Keywords:*
Strombolian activity
magma vesiculation
infrasound
conduit dynamics
explosive volcanism
bubble size distribution

ABSTRACT

Explosive activity at Stromboli is explained in terms of dynamics of large gas bubbles that ascend in the magma conduit and burst at the free surface generating acoustic pressure that propagates as infrasonic signals in the atmosphere. The rate and the amplitude of the infrasonic activity is directly linked to the rate and the overpressure of the bursting gas bubbles and thus reflects the rate at which magma column degasses under non-equilibrium pressure conditions.

We investigate the link between explosive degassing and magma vesiculation by comparing the rate of infrasonic activity with the bubble size distributions (BSDs) of scoria clasts collected during several days of explosive activity at Stromboli. BSDs of scoria show a characteristic power law distribution, which reflect a gas bubble concentration mainly controlled by a combined process of bubble nucleation and coalescence.

The cumulative distribution of the infrasonic pressure follows two power laws, indicating a clear separation between the frequent, but weak, bursting of small gas bubbles (puffing) and the more energetic explosions of large gas slugs. The exponents of power laws derived for puffing and explosive infrasonic activity show strongly correlated (0.96) changes with time indicating that when the puffing rate is high, the number of energetic explosions is also elevated. This correlation suggests that both puffing and explosive activity are driven by the same magma degassing dynamics. In addition, changes of both infrasonic power law exponents are very well correlated (0.92 with puffing and 0.87 with explosions) with variations of the BSD exponents of the scoria clasts, providing evidence of the strong interplay between scoria vesiculation and magma explosivity. Our analysis indicates that variable magma vesiculation regimes recorded in the scoria correlate with the event number and energy of the explosive activity. We propose that monitoring infrasound on active volcanoes may be an alternative way to look at the vesiculation process in open conduit systems.



## 1. Introduction

Volcanic eruptions involve the exsolution, growth and expansion of a gas phase during magma ascent towards the Earth's surface, resulting in large variations of the magma's rheological properties and changes in its dynamical regime when fragmentation occurs (Jaupart and Tait, 1990). Problems linked to the vesiculation and fragmentation of magma have long challenged geologists: vesiculation and degassing are the primary trigger of volcanic eruptions and amongst the most important factors controlling the rheology of magmas (Sparks, 1978; Gardner et al., 1996; Manga et al., 1998; Papale, 1999; Giordano and Dingwell, 2003). When magma ascends toward the surface, pressure in the column decreases, volatile solubility decreases and upon supersaturation, bubble nucleation begins.

Bubbles in fragmented, erupted magmas are usually regarded as a mixture of gases that nucleates and grows by decompression and diffusion in magma chambers, and/or during their ascent in the conduit (Sparks and Brazier, 1992; Mangan et al., 1993; Blower et al., 2002). The dynamics of vesiculation cannot be directly observed in the magmatic column, so the process of bubble nucleation and growth must be inferred from secondary sources such as theoretical studies (Proussevitch and Sahagian, 1998), laboratory investigations (Jaupart and Vergniolle, 1989; Mader et al., 1994; Blower et al., 2001; Namiki et al., 2003) and textural analysis of volcanic rocks (Cashman et al., 1994; Klug and Cashman, 1996; Mangan and Cashman, 1996). Vesiculation is frequently studied using bubble size distributions (BSD) and the integrated cumulative frequency–bubble size distribution of volcanic rocks (see, for example, Mangan et al., 1993; Gaonac'h et al., 1996a; Klug et al., 2002). According to their bubble size distribution, scoria and lava samples contain information on vesiculation during volcanic eruptions or magma degassing and allow us to infer magma chamber processes and conduit dynamics.

The present work combines textural analysis of scoria samples collected during the persistent explosive activity at Stromboli volcano (Aeolian Islands, Italy) with infrasonic activity recorded during the same period of the scoria collection.

* Corresponding author.
*E-mail address:* maurizio.ripepe@unifi.it (M. Ripepe).

0012-821X/$ – see front matter © 2010 Elsevier B.V. All rights reserved.
doi:10.1016/j.epsl.2010.01.018

Explosive activity is evidence that part of the exsolved gas leaves the magma column in non-equilibrium pressure conditions. The bursting of gas bubbles is recorded as acoustic pressure which propagates in the atmosphere as an infrasonic wave. The infrasonic amplitude is a function of gas overpressure and bubble volume (Vergniolle and Brandeis, 1996; James et al., 2009).

At Stromboli, infrasound reveals that Strombolian explosions are associated with a persistent background activity of small (0.5–6 Pa) pressure transients occurring every ~2 s (Ripepe et al., 1996). This infrasonic activity represents the bursting of small gas bubbles in overpressurized conditions (puffing) and involves, at smaller scale but higher rate, the same magma breaking mechanisms (or shallow magma fragmentation) as the larger explosive events.

This persistent but weak gas bursting activity (puffing) accounts for ~50% of the total gas budget at Stromboli volcano (Harris and Ripepe, 2007; Ripepe et al., 2008) and can be considered as the active (non-equilibrium) counterpart of the passive magma degassing, which is silent in the infrasonic range (Harris and Ripepe, 2007). Considering that another ~10% of the gas budget is released by Strombolian explosive activity (Allard et al., 1994; Burton et al., 2007), more than ~60% of the total gas at Stromboli leaves the magma column in overpressurized conditions (Ripepe et al., 2008) and thus forms a major proportion of the degassing dynamics.

We compare the cumulative distribution of infrasonic pressures with the cumulative distribution of bubble sizes in scoria to investigate if variations in vesiculation measured in scoria clasts are related to variations in the degassing rate of the magma column both as puffing and as explosions. Our hypothesis is that these two processes reflect different aspects of the degassing process, where infrasound is the indirect but continuous measure of the magma column degassing in overpressurized conditions, while scoria clasts represent the discrete and discontinuous evidence of magma vesiculation.

We show that the correlation of the two datasets can provide important information about the vesiculation process in magmas.

## 2. BSD analysis on X-ray tomographic images

Quantitative data on the number, shape and size distributions of bubbles in volcanic scoria provide useful information about magma vesiculation processes as these parameters are directly related to the kinetics of bubble nucleation and growth, and/or to the influence of vesiculation rate on magma fragmentation (Cashman et al., 1994; Mangan and Cashman, 1996). BSD allows us to infer which processes (nucleation, diffusive growth, expansion or coalescence) dominate during magma fragmentation.

Quantitative analysis of bubble textures were obtained by processing 2D slices of tomographic images (~$1.5 \times 1.5$ cm$^2$) of scoria products collected during normal Strombolian activity at Stromboli volcano in 2004, 2005 and 2006. These images were obtained from X-ray tomographic analysis performed at the SYRMEP beamline of Elettra Sincrotrone Trieste in Basovizza (Trieste, Italy).

X-ray computed microtomography (μCT) is a technique that can be used for imaging the inner 3D structure of volcanic rocks and measuring their physical properties (Fig. 1). This method is non-destructive, and provides large quantities of 2D and 3D micro-structural information of porous materials with micron-scale resolution (Proussevitch et al., 2007; Bai et al., 2008; Okumura et al., 2008; Polacci et al., 2009). Tomographic scans of each reconstructed scoria volume were analyzed with the software ImageJ (Abramoff et al., 2004), each 3D scan consisting of 200–400 2D slices, with a pixel size of 9 or 14 μm. For further information on the μCT technique and experimental conditions at the SYRMEP beamline refer to Polacci et al. (2006, 2009).

We processed images of 11 tomographic volumes related to scoria clasts collected during different periods of explosive activity at Stromboli. All samples were collected at the crater rim just after they were ejected and, therefore, they are very well defined both in time and space; for each scoria clast we know exactly the date, the crater from which they were ejected and the associated infrasonic activity.

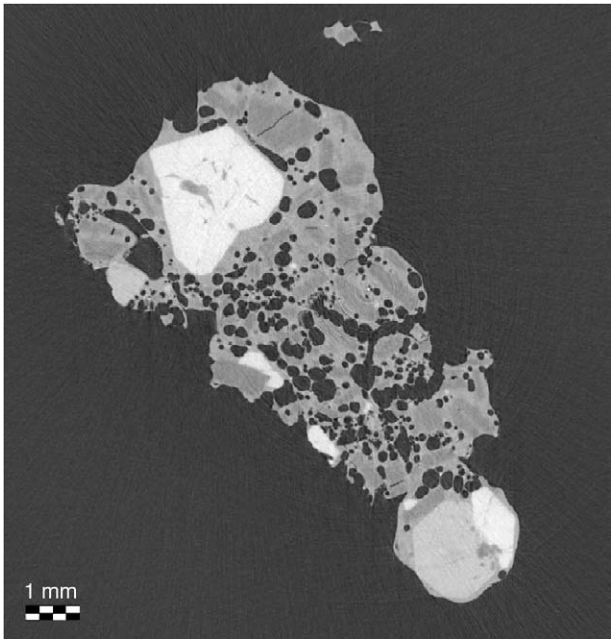


**Fig. 1.** One slice of 778 × 778 pixels, (1 pixel = 14 μm) of the scoria 20041221, obtained via synchrotron X-ray computed microtomography (μCT). Black holes are bubbles, light grey is glass and crystals are dark grey or white.

The tomographic images of scoria are characterized by small spherical or sub-spherical bubbles. All but one of the analyzed scoria samples show no textural and morphological features typical of post-fragmentation degassing (e.g., a vesicularity gradient) and do not contain very small crystals with irregular and uneven edges characteristic of secondary fragmentation (Taddeucci et al., 2004). Therefore, we consider that these scoria are representative of the state of the magma within the conduit before fragmentation. The scoria sample of April 14, 2006 shows a vesicularity gradient and was analyzed from top to bottom in three different tomographic runs (top, middle, and bottom), each run representing a different part of the sample.

Generally, 2D analysis of BSD is calculated on several images with different magnification of few (4–5) thin sections of the same scoria (e.g., Mangan and Cashman, 1996). According to the magnification level, each image contains different ranges of bubble sizes. The BSD calculated with this 2D procedure is strongly limited by the magnification used, by the possible presence of elongated (non-spherical) bubbles and, even if bubbles are spherical, by the disagreement between the diameter of the bubble on the slice plane and the true bubble diameter (stereology problem). Recently, all these problems have been solved by the use of 3D analysis on the tomographic 3D reconstruction of the scoria image (e.g., Polacci et al., 2009). However, this tomographic procedure is very time-demanding (4–5 days for a single scoria) and it is still not of common use. A comparison between 3D tomographic volumes and 2D processing of the same sample revealed that vesicularity and connectivity values are in quite good agreement to each other (Polacci et al., 2009). We thus preferred to apply the 2D technique to estimate BSD values, which can be better compared to previous vesicularity analyses. In addition, here we are interested in changes of magma vesicularity with time rather than a thorough description of the BSD of scoria samples at Stromboli, which can be found in Polacci et al. (2009).

In our 2D technique, resolution of the smallest bubbles is not limited by the image magnification used in classic thin-section analysis and the presence of elongated bubbles is partially compensated by the high number of slices (200–400) used for the same scoria.

Each pixel in the tomographic image was reduced to 1 (solid) or 0 (void), and all the voids were automatically identified by a specifically written MatLab program (Colò, 2007). Our software discriminates between internal and external bubble boundaries, where external boundaries of bubbles represent the external boundaries of the scoria sample and thus open bubbles, which are ignored. The distribution of bubble areas and the cumulative bubble size distributions were computed using a maximum bubble size threshold of $4\times10^{-2}$ mm$^2$ equivalent to a radius of 0.11 mm (12–8 pixels according to the image resolution) to avoid bubbles as large as the sample itself. As a consequence the analyzed BSD range from $10^{-2}$ mm$^2$ (0.05 mm is 6 or 4 pixels) to $10^{-3.6}$ mm$^2$ (0.009 mm that is 1 or 0.6 pixels) (the minimum bubble area observed). These procedures allow us to quickly analyze several hundreds of images for each sample, many more than possible using conventional thin-section analysis.

In order to have a more reliable representation of the bubbles within the entire scoria volume, the BSD was calculated as the total number of bubbles present in several slices of the same scoria. To avoid counting the same bubble several times, we considered only slices at a distance of ~0.11 mm which, depending on the pixel size of the X-ray camera, coincides with the largest bubble radius and is equivalent to processing one slice every ten. For each scoria we analyzed 20–40 slices at once and automatically calculated the 2D distribution of the cumulative BSD. Finally, the total number of bubbles was normalized to the total area of the slices used, and the results converted into a bubble number density (BND). Stability of this procedure is quite high; by changing the position of the first slice within the image stack, we observed a variability of only 10% in the calculated BSDs slopes and BND value.

## 3. Power law BSD in scoria

Most of the scoria sampled on volcanoes show unimodal, logarithmic and power law BSDs reflecting different vesiculation processes (Toramaru, 1990; Mangan et al., 1993; Gaonac'h et al., 1996b). The unimodal distribution has been explained by a single event of bubble nucleation (Toramaru, 1989) while the exponential distribution has been interpreted as the result of a continuous bubble nucleation in a steady-state regime (Marsh, 1988).

All the cumulative BSDs measured in our scoria follow a power law $N(>A)=cA^{-b}$, where $N$ is the number of bubbles greater than area $A$, $c$ is a constant and $b$ is the exponent of the distribution (Turcotte, 1986). A power law BSD indicates that bubble growth in the scoria follows a scale-invariant process and that there is no characteristic bubble size in the sample. However, the origin of the power law distribution is still not clearly understood (c.f., Gaonac'h et al., 1996a; Blower et al., 2002). The slope of the distribution represents the exponent of the power law $b$ (or average fractal dimension) and contains information on the relative distribution of the bubble population that is directly linked to the dynamics of the vesiculation process (Gaonac'h et al., 1996b; Blower et al., 2001; Gaonac'h et al., 2005).

A steep BSD power law will have a large exponent, indicating a scoria rich in small bubbles. When the exponent $b$ approaches zero, the BSD becomes flatter, indicating a more uniform distribution and a relative increase in the number of large bubbles in the sample. In terms of magma vesiculation, small bubbles represent the nucleation process while large bubbles reflect bubble growth by decompression (Mangan and Cashman, 1996; Blower et al., 2001) or by cascade coalescence (Gaonac'h et al., 1996a). BSDs with steep slopes, and thus rich in small bubbles, reflect a volatile-rich magma under violent decompression process (Blower et al., 2002). Therefore, monitoring changes of the power law exponent (calculated always within the same BSD range) will document the variation and evolution of the magma vesiculation process.

All the calculated BSDs follow similar power laws with 2D exponents well constrained in a range from 0.4 to 0.8 (Table 1, Fig. 2a). The exponents of the cumulative BSD for the scoria sample of April 14, 2006 analyzed in three different tomographic runs, are very similar to each other ~0.52, (Table 1). This demonstrates that even a small subsection of a sample is representative of the magma from which it comes, as the scale-invariant power law suggests.

The 2D area-dependent distribution $N(>A)$ were converted into the 3D radius distribution $N(>R)$ by using the expression $b_{3D}=2b_{2D}+1$, where $b_{2D}$ is the exponent of the 2D area distribution of the bubble and and $b_{3D}$ is the 3D bubble radius distribution, respectively (Blower et al., 2002). We found that the 3D-converted BSD exponents range from 1.8 to 2.6 (Table 1). Most BSDs of scoria from basaltic eruptions follow a power law distribution with the exponent ranging from 2.3 to 3 (Blower et al., 2002), which were interpreted in terms of multiple nucleation events during constant decompression growth (Blower et al., 2001), or as the evidence of efficient bubble coalescence (Gaonac'h et al., 1996a).

An increase in the number of nucleation events in a rapid decompression regime will result in a large number of small bubbles and then in a progressively steeper BSD (Blower et al., 2002). Our BSDs have low exponents (1.8–2.6) indicating a relatively large contribution of big bubbles ($10^{-2}$ mm$^2$) and a vesiculation process dominated by efficient bubble growth or coalescence. This vesiculation regime agrees well with our understanding of the moderate explosive activity of Stromboli being driven by large gas bubbles growing in a quasi-static magma column.

## 4. Infrasound of a degassing magma conduit

Volcanic activity at Stromboli produces infrasonic signals whose amplitude and occurrence rate reflect gas overpressure magnitude and bubble bursting rates. Pressure transients were recorded by a 5 element small aperture (200 m) infrasonic array deployed with an L shape of 200 m length at a short distance (<450 m) from the summit craters. Multi-channel semblance processing allows us to identify and locate every single infrasonic event produced by this gas bursting activity (Ripepe and Marchetti, 2002).

The infrasonic amplitude distributions (IADs) were calculated as the cumulative number of acoustic pressure events $N(>Pa)$ recorded by the array in 24 hour time intervals for the same days as the scoria were sampled. For each of the seven analyzed days, IADs show two

**Table 1**
Sample name indicate the sampling day in the year, month and day (e.g., 20060414 was sampled on April 14th of 2006). The sample 20060414 was analyzed in three different runs (t = top, m = middle, b = bottom) because of its vesicularity gradient, while a and c indicate two different scoria sampled in the same day. $b_{2D}$ and $b_{3D}$ contain the 2D and 3D scoria exponents, respectively. BND indicates the bubble number density expressed in cm$^{-2}$. $E_D$ and $E_X$ are the exponents of the infrasonic amplitude distribution (IAD) for puffing and explosion, respectively. IND represents the sum of the average hourly pressure released over the 24 h of each sampling day (Pa/h).

| Sample | $b_{2D}$ | $b_{3D}$ | BND | $E_D$ | $E_X$ | IND |
|---|---|---|---|---|---|---|
| 20041221 | 0.57 | 2.14 | 507 | 1.33 | 1.17 | 119 |
| 20050303 | 0.49 | 1.98 | 680 | 2.81 | 0.98 | 124 |
| 20050917 | 0.42 | 1.84 | 767 | 2.97 | 0.28 | 854 |
| 20060414 t | 0.52 | 2.04 | 263 | 2.34 | 0.86 | 870 |
| 20060414 m | 0.50 | 2.00 | 197 | 2.34 | 0.86 | 870 |
| 20060414 b | 0.54 | 2.08 | 218 | 2.34 | 0.86 | 870 |
| 20060415 | 0.56 | 2.12 | 553 | 2.28 | 1.31 | 784 |
| 20060522 | 0.46 | 1.92 | 552 | 3.59 | 1.00 | 1025 |
| 20060524 | 0.69 | 2.38 | 1563 | 2.31 | 2.03 | 294 |
| 20060525 a | 0.84 | 2.68 | 1310 | 2.97 | 1.86 | 286 |
| 20060525 c | 0.64 | 2.29 | 1473 | 2.97 | 1.86 | 286 |

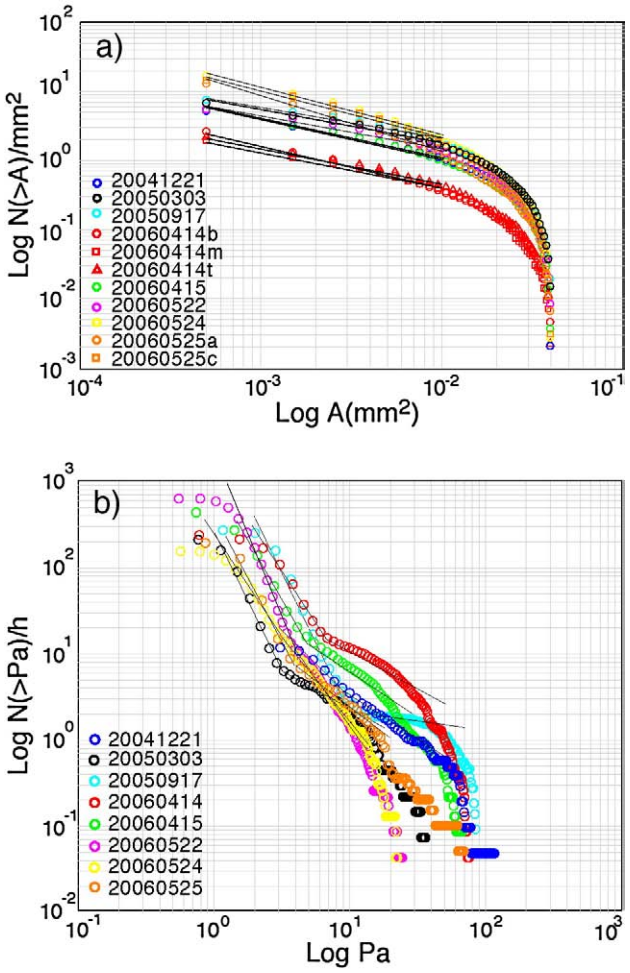


**Fig. 2.** a) Cumulative distributions of apparent bubble areas of the scoria sampled during different days of explosive degassing at Stromboli. BSD is calculated as a function of the area of bubbles in $mm^2$. The sample name corresponds to the sampling day. BSDs in the range from $10^{-2}$ $mm^2$ to $10^{-3.6}$ $mm^2$ show power law distributions with exponents ranging from 0.4 to 0.8. b) Cumulative distributions of infrasonic amplitude (IAD) calculated during the same days as the scoria sampling. Acoustic pressure (Pa) refers to the amplitude of the infrasonic waves recorded at the array, at ~450 m from the craters. The time interval considered is 24 h long and IADs are represented as the number of infrasonic events per hour. IADs show two different power law segments, with a stable inflection point at 3–6 Pa, which separates puffing (~<5 Pa) from explosions (~>5 Pa).

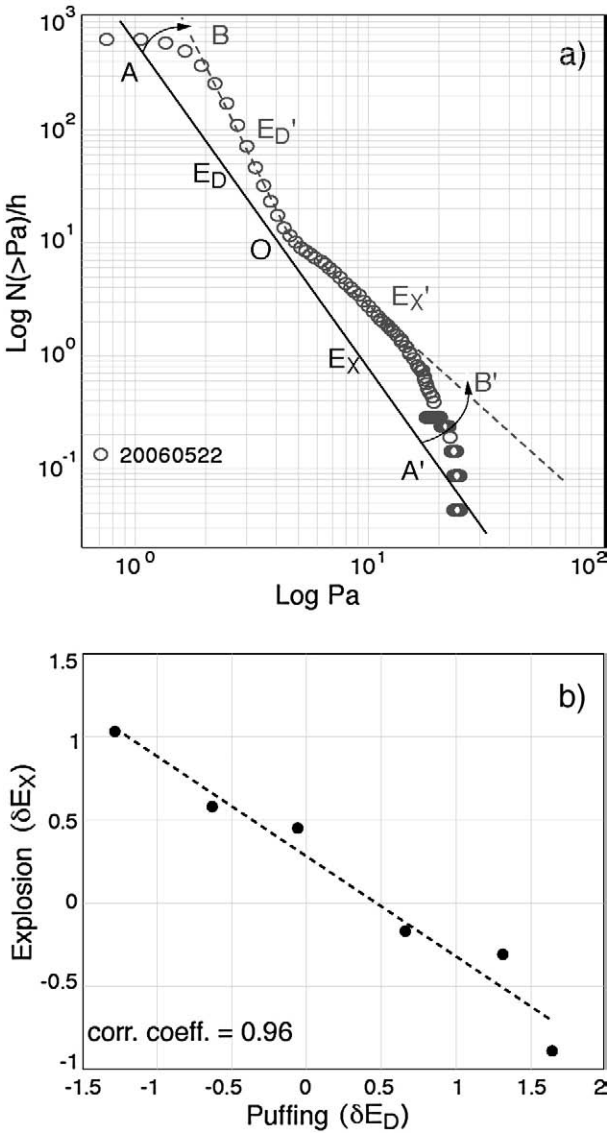


**Fig. 3.** a) Power law of the cumulative infrasonic amplitude distribution (IAD) for a variable explosive degassing rate. AA′ represents an expected IAD with a single power law indicating a common degassing rate for puffing and explosions; BOB′ reflects the response of the IAD to an increase in the degassing rate, which should induce a higher number of small infrasonic transients (BO) and more vigorous explosions (OB′). $E_D$ is the exponent produced by the overall degassing activity. Segments BO and OB′ represent the exponents $E_D$ and $E_X$ of the IAD for puffing and explosion, respectively. O indicates the inflection point around which the two segments, $E_D$ and $E_X$ rotate. b) Relative changes of IAD exponents for puffing ($\delta E_D = E_D(i) - E_D(i-1)$) and explosion ($\delta E_X = E_X(i) - E_X(i-1)$ ($i = 1,2,..7$)). Relative changes in the measured IAD exponents show a good inverse correlation (0.96) indicating that an increase in the IAD exponent of puffing (IAD~<5 Pa) is associated to a decrease of the IAD exponent calculated for the explosive activity (IAD~>5 Pa). This behaviour is consistent with the degassing model proposed in Fig. 3a where the rate and amplitude of infrasonic activity is controlled by the degassing rate.

power law distributions (Fig. 2b), which have an inflection point at around 3–6 Pa. The two power law IAD segments suggest that infrasound is produced by a gas bursting process acting at two different rates. For IAD<~5 Pa ($E_D$) the high rate of small acoustic amplitude represents the small gas bursting activity (puffing), while for IAD>~5 Pa ($E_X$) the less frequent but more vigorous acoustic pressure reflects the Strombolian explosive activity (Fig. 3a).

The presence of a double IAD power law suggests that there is no smooth transition between the acoustic pressure released during explosive and puffing activity, but the two degassing regimes remain very well separated in time. This behaviour is consistent with the IAD calculated for a one year-long period during 2003–2004 (Marchetti et al., 2006; Ripepe et al., 2007).

The crossing point between the two IAD trends suggests the boundary between puffing and explosive activity. This limit (at 3–6 Pa) can be considered to be quite stable when compared to the full range (from 0.5 to 100 Pa) of the recorded infrasonic amplitudes and suggests the existence of a threshold condition between puffing and explosive dynamics. Recent experiments show that in a stationary flow regime the acoustic pressure generated by bubble bursting is a function of the gas mass (James et al., 2009). However, acoustic pressure drastically drops below a gas mass threshold which separates two regions with different bursting vigour: the energetic explosion of large slugs and the weak bursting of small gas bubbles. According to James et al. (2009), this gas mass threshold at Stromboli should be of ~10 kg, which coincides well with the mean gas mass (~30 kg) of a single gas puff estimated by thermal analysis (Harris and Ripepe, 2007). Our infrasonic data indicate that this gas mass threshold defines also a net change in the occurrence rate between two degassing styles.

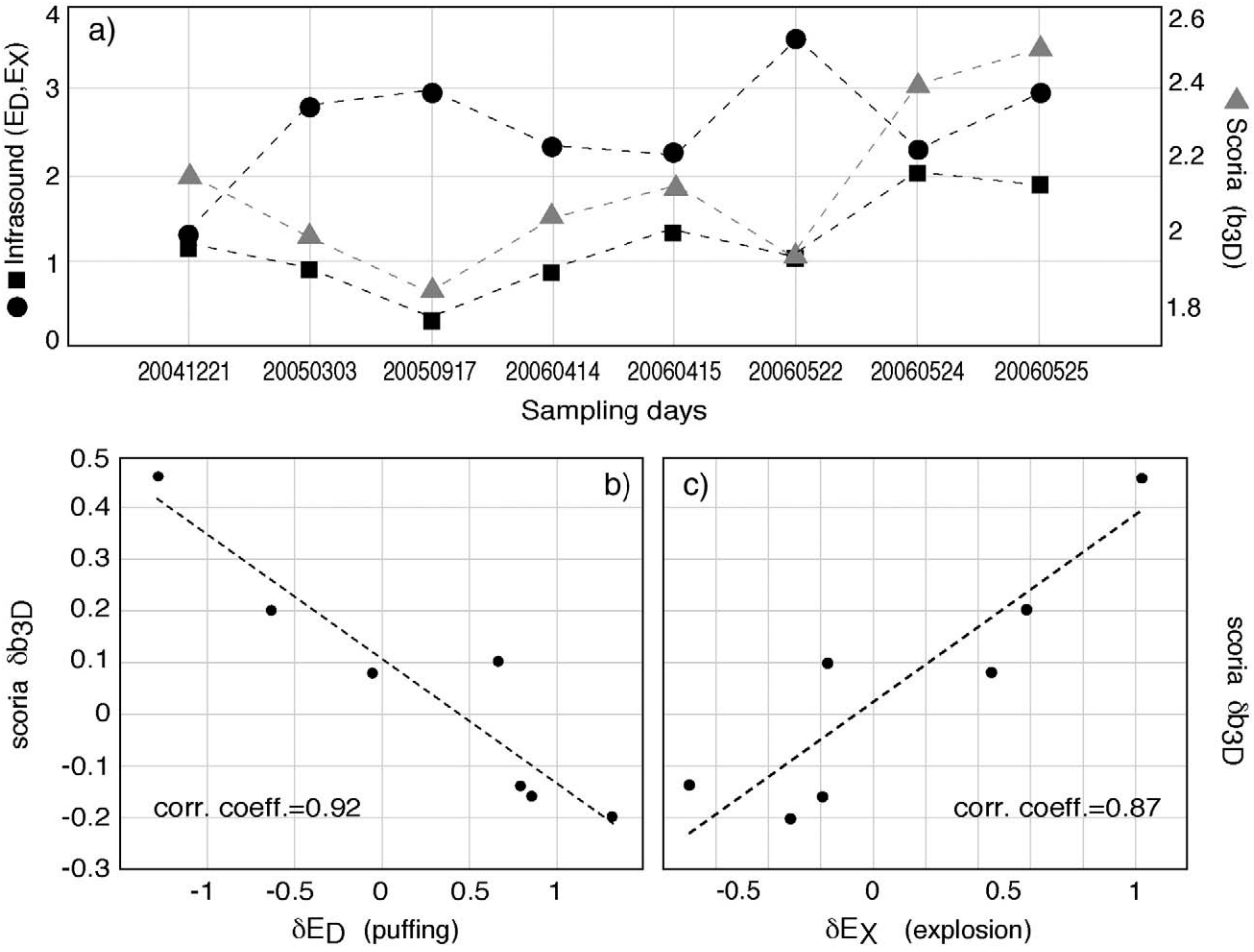


**Fig. 4.** a) Linked variation of the exponent $b_{3D}$ for the scoria (grey triangles) with the exponents $E_X$ and $E_D$ of the acoustic pressure generated by explosions (black squares) and puffing (black circles), respectively. Relative changes of scoria $\delta b_{3D}$ show (b) a strong inverse relationship with changes $\delta E_D$ in the rate of puffing activity (correlation coefficient 0.92) and (c) are directly correlated (correlation coefficient 0.87) with changes $\delta E_X$ in the exponent of the explosive activity, reflecting the strong link between the vesiculation process and infrasonic activity.

## 5. Changes of infrasound and scoria distributions

The exponents of puffing ($E_D$) and explosions ($E_X$) are not stable in time (Fig. 4a) reflecting variations in both amplitude and rate of acoustic pressure. Stable exponents would indicate that the physical process driving the two degassing regimes remains in a steady-state condition. Conversely, variations in the exponents with time will reflect changes in the rate at which gas is released by bubble bursting (Ripepe et al., 2007) (Fig. 3a).

We observe that relative variations of both puffing $\delta E_D = E_D(i) - E_D(i-1)$ and explosion $\delta E_X = E_X(i) - E_X(i-1)$ IAD exponents (where $i = 1,2,..7$ indicates each of the 7 analyzed days) change together following a strong (0.96) linear ($\delta E_X = -0.66\delta E_D + 0.28$) inverse correlation (Fig. 3b). This coupled behaviour of the exponents supports the hypothesis that puffing and explosions are responding to the same process. In addition, the slope of the linear trend (0.66), between the relative changes of puffing ($\delta E_D$) and explosion ($\delta E_X$) IAD exponents, indicates that puffing rate is growing 1.5 times faster than explosions.

This coupling between the rate of puffing and explosions at Stromboli was reported previously and was explained as a common response to the general increase of gas content in the magma column (Ripepe et al., 2002, 2008).

Because the boundary between the two segments of the IAD is stable, an increase of explosions with larger infrasonic pressures will generate a negative $\delta E_X$ for the IAD exponent (Fig. 3a). Similarly, an increase in the bursting rate of small bubbles, and thus in the number of small infrasonic amplitude events will lead to a positive $\delta E_D$.

Hence, changes in the IAD exponents (Fig. 3b) can be interpreted to reflect changes in the quantity of exsolved gas from the magma column, where large quantities of overpressurized gas induce a higher active degassing rate ($\delta E_D > 0$) and a stronger explosive activity ($\delta E_X < 0$).

The BSDs of the scoria clasts and the IADs of the infrasonic activity follow power law distributions that are not stable in time but indicate changes in the vesiculation process (BSD) and in the rate of overpressurized (explosive) magma degassing (IAD). The two distributions show (Fig. 4a) well correlated variations suggesting a strong interaction between magma vesiculation and explosive degassing rate. When the exponent of the BSD ($b_{3D}$) increases the exponent of the IAD associated with explosions ($E_X$) also increases, while the exponent relative to puffing ($E_D$) decreases (Fig. 4a).

The coupling between infrasound and scoria is better evidenced when we consider relative changes of the exponents. Relative change in the BSD exponent, defined as $\delta b_{3D} = b_{3D}(i) - b_{3D}(i-1)$, reveals high correlation coefficients with both IAD exponents $\delta E_D$ for puffing (0.92) and $\delta E_X$ for explosion (0.87) evidencing the strong coupling between the scoria vesiculation and the explosive magma degassing process (Fig. 4b and c).

During the high explosive degassing regime, the rate of puffing increases ($\delta E_D > 0$) and the acoustic amplitude of the explosions becomes larger ($\delta E_X < 0$) while the BSD exponent of the scoria becomes flatter ($\delta b_{3D} < 0$). By contrast, during the low degassing phase, puffing rate decreases ($\delta E_D < 0$) and the vigour of the explosions decreases ($\delta E_X > 0$) while the BSD exponent of the scoria becomes steeper ($\delta b_{3D} > 0$).

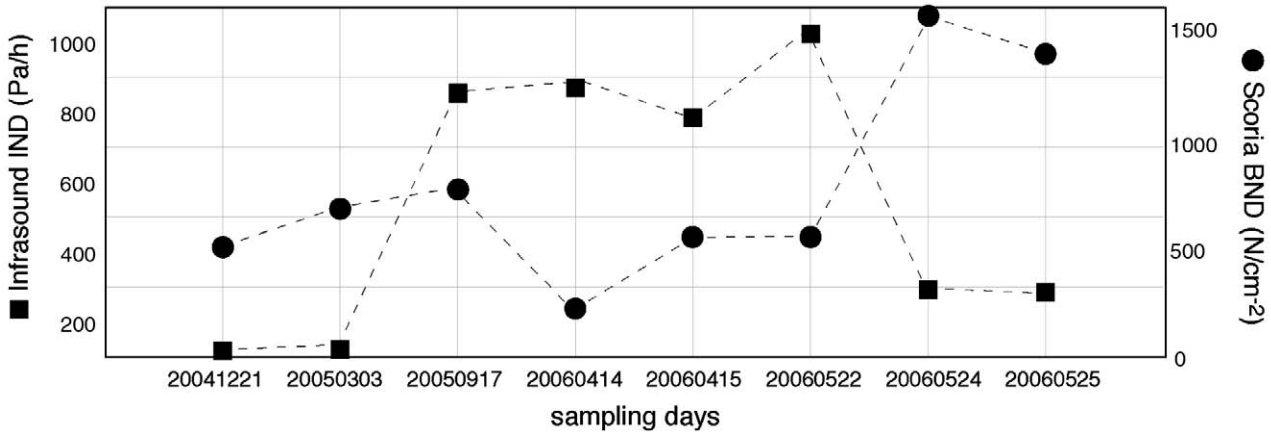


**Fig. 5.** The total number of bubbles (BND in $cm^{-2}$) in each scoria is compared with the overall level of explosive degassing activity, represented by the total number of infrasonic amplitudes (IND) and calculated as the area below the IAD of Fig. 2a. Small BND reflects a large contribution of big bubbles to the scoria vesiculation and, in general, correlates with a period of high infrasonic activity (large IND) and with periods of high explosive degassing regime. This correlation is good enough (correlation coefficient 0.61) to support an explosive degassing model controlled by a bubble accumulation process.

## 6. Discussion

Infrasound demonstrates that a significant part (~60%) of magma degassing occurs at non-equilibrium conditions. Explosive and puffing activity represent two aspects of the same explosive degassing mechanism acting at different scales (Ripepe et al., 2002; Harris and Ripepe, 2007; Ripepe et al., 2008; James et al., 2009). Our results suggest that variations in the explosive degassing are printed in the vesiculated scoria and that both are controlled by the same gas discharge mechanism of the magma column.

In a model where gas bubbles nucleate continuously and grow by decompression, the power law exponent of BSD is explained in terms of the number of nucleation events (Blower et al., 2002). A steeper BSD reflects a vesiculation process dominated by small bubbles and is evidence for a large number of nucleation events during fast decompression of volatile-rich magma. Moreover, vesiculation controlled by a large population of small bubbles will display a large bubble number density (BND). At Stromboli, scoria collected during explosive activity show vesiculation characterized by a relatively large population of big bubbles, and then by an overall small bubble density (BND), indicating an efficient gas accumulation mechanism.

However, our scoria show one order of magnitude variability in the BND (Fig. 2a) a large range in vesicularity. In general, the scoria with the smallest BND have been collected during high infrasonic activity, as indicated by the overall increase in the total infrasonic amplitude (IND) calculated as the acoustic pressure released in one hour (Fig. 5). In contrast, scoria with larger BND correlate with a period of low infrasonic activity (Fig. 5). Therefore, a frequent and more explosive degassing regime is associated with a relatively coarse bulk vesiculation, whilst smaller bubbles dominate during weak explosive periods with low degassing rates. This correlation between explosive degassing and magma vesiculation is evidence of gas-driven dynamics and it suggests that explosive dynamics and vesiculation process are dominated by an efficient bubble growth process.

Changes in the BSD power law exponent as a function of volatile exsolution has been observed in a thermally-driven convecting viscous layer (Namiki et al., 2003). In their experiment, a bubble size distribution with a small exponent, hence dominated by large bubbles, is observed during the volume expansion of the convective layer. When the convective layer shrinks due to reduced nucleation, the BSD shows large exponents reflecting a small bubble-dominated vesiculation.

Explosive activity at Stromboli is the evidence for efficient conduit convection, in which gas-rich magma ascends, degasses and sinks within the conduit either as discrete batches or as a continuous cycle (Harris and Stevenson, 1997). In a convecting magma conduit, the central part of the ascending magma column is less dense and contains more bubbles than the outer sinking area of degassed, more dense, magma (Kazahaya et al., 1994; Stevenson and Blake, 1998). Increasing the volatiles in a magma column leads to a decrease of the local mean density in the bubble-rich magma layer and to a more efficient convection. This will also induce a local increase of the effective viscosity up to several orders of magnitude (Phillips et al., 1995; Rust and Manga, 2002), creating in a quasi-static magma column more-favorable conditions to trap and grow larger gas bubbles by coalescence (Namiki et al., 2003).

We suggest that a density-driven convective magma column can explain the observed link between the rate of the explosive degassing activity and the large bubble-dominated magma vesiculation. High volatile content will promote a high density contrast and the proper viscosity condition to enhance the growth of large, meter-size bubbles and slugs, leading to a general increase in the explosive degassing.

## 7. Conclusions

We compared bubble size distributions (BSDs) measured in scoria clasts ejected during normal explosive activity of Stromboli with the amplitude distributions of infrasonic signals (IADs) produced by the puffing and explosive activity during the same days. BSDs and IADs follow power laws which vary in time reflecting changes in both the vesiculation process and in the explosive degassing.

These correlations suggest that scoria vesiculation and infrasonic pressures are linked to the same variations in the gas content in the magma column. Increasing gas content not only involves more vigorous and energetic volcanic activity, but it also produces a more-developed magma vesiculation.

Our results suggest a way to look at infrasound activity and vesiculation processes together as linked to the same changes in the magma degassing process. If sampling volcanic products is sometimes impossible, infrasound may be an indirect but continuous way to monitor vesiculation of the upper part of the magmatic column at open conduit volcanoes like Stromboli. Infrasound can be a useful technique for monitoring changes in vesiculation of a magmatic conduit and a new key for interpreting the vesiculation process in terms of volcanic explosivity.

## Acknowledgements

This manuscript has been largely improved by the constructive reviews of Kathy Cashman and Mike James which have helped us to

refine our primitive ideas on magma vesiculation and degassing process. We thank Lucia Mancini and the SYRMEP Group for help in the acquisition and elaboration of the tomographic scans.

## References


Abramoff, M.D., Magelhaes, P.J., Ram, S.J., 2004. Image processing with Image. J. Biophot. Int. 11, 36–42.

Allard, P., Carbonelle, J., Metrich, N., Loyer, H., Zettowoog, P., 1994. Sulphur output and magma degassing budget of Stromboli volcano. Nature 368, 326–330.

Bai, L., Baker, D.R., Rivers, M., 2008. Experimental study of bubble growth in Stromboli basalt melts at 1 atmosphere. Earth Planet. Sci. Lett. 267, 533–547. doi:10.1016/j.epsl.2007.11.063.

Blower, J.D., Keating, J.P., Mader, H.M., Phillips, J.C., 2001. Inferring volcanic degassing processes from vesicle size distributions. Geophys. Res. Lett. 28, 347–350. doi:10.1029/2000GL012188.

Blower, J.D., Keating, J.P., Mader, H.M., Phillips, J.C., 2002. The evolution of bubble size distributions in volcanic eruptions. J. Volcanol. Geotherm. Res. 120, 1–23.

Burton, M., Allard, P., Murè, F., La Spina, A., 2007. Magmatic gas composition reveals the source depth of slug-driven Strombolian activity. Science 317, 227. doi:10.1126/science.1141900.

Cashman, K.V., Mangan, M.T., Newman, S., 1994. Surface degassing and modifications to vesicle size distributions in active basalt flows. J. Volcanol. Geotherm. Res. 61, 45–68.

Colò, L., 2007. Master Thesis, Analisi dei processi di degassamento legati all'attività infrasonica nei vulcani a condotto aperto.

Gaonac'h, H., Lovejoy, S., Schertzer, D., 2005. Scaling vesicle distributions and volcanic eruptions. Bull. Volcanol. 67, 350–357.

Gaonac'h, H., Lovejoy, S., Stix, J., Scherzter, D., 1996a. A scaling growth model for bubbles in basaltic lava flows. Earth Placet. Sci. Lett. 139, 395–409.

Gaonac'h, H., Stix, J., Lovejoy, S., 1996b. Scaling effects on vesicle shape, size and heterogeneity of lavas from Mount Etna. J. Volcanol. Geotherm. Res. 74, 131–153.

Gardner, J.E., Thomas, R.M.E., Jaupart, C., Tait, S., 1996. Fragmentation of magma during Plinian volcanic eruptions. Bull. Volcanol. 58, 144–162.

Giordano, D., Dingwell, D.B., 2003. Non-Arrhenian multicomponent melt viscosity: a model. Earth Planet. Sci. Lett. 208, 337–349.

Harris, A., Ripepe, M., 2007. Temperature and dynamics of degassing at Stromboli. J. Geophys. Res. 112, B03205. doi:10.1029/2006JB004393.

Harris, A.J.L., Stevenson, D.S., 1997. Thermal observations of degassing open conduits and fumaroles at Stromboli and Vulcano using remotely sensed data. J. Volcanol. Geothem. Res. 76, 175–198.

James, M.R., Lane, S.J., Wilson, L., Corder, S.B., 2009. Degassing at low magma-viscosity volcanoes: quantifying the transition between passive bubble-burst and Strombolian eruption. J. Volcanol. Geotherm. Res. 180, 81–88.

Jaupart, C., Tait, S., 1990. Dynamics of eruptive phenomena in: Modern Methods in Igneous Petrology. Min. Soc. Am. Rev. 24, 213–238.

Jaupart, C., Vergniolle, S., 1989. The generation and collapse of a foam layer at the roof of a basaltic magma chamber. J. Fluid. Mech. 203, 347–380.

Kazahaya, K., Shinohara, H., Saito, G., 1994. Excessive degassing of Izu-Oshima volcano-magma convection in a conduit. Bull. Volcanol. 56, 207–216.

Klug, C., Cashman, K.V., 1996. Permeability development in vesiculating magmas: implications for fragmentation. Bull. Volcanol. 58, 87–100.

Klug, C., Cashman, K.V., Bacon, C., 2002. Structure and physical characteristics of pumice from the climactic eruption of Mount Mazama (Crater Lake). Oregon. Bull. Volcanol. 64, 486–501.

Mader, H.M., Zhang, Y., Phillips, C.J., Sparks, R.S.J., Sturtevant, B., Stolper, E., 1994. Experimental simulation of explosive degassing of magma. Nature 372, 85–88.

Manga, M., Castro, J., Cashman, K., 1998. Rheology of bubble bearing magmas. J. Volcanol. Geotherm. Res. 87, 15–28.

Mangan, M.T., Cashman, K.V., 1996. The structure of basaltic scoria and reticulite and inferences for vesiculation, foam formation, and fragmentation in lava fountains. J. Volcanol Geotherm. Res. 73, 1–18.

Mangan, M.T., Cashman, K.V., Newman, S., 1993. Vesiculation of basaltic magma during eruption. Geology 21, 157–160.

Marchetti, E., Ripepe, M., Ulivieri, G., 2006. Degassing Dynamics at Stromboli Volcano: Insights from Infrasonic Activity. International Workshop: Physics of Fluid Oscillations in Volcanic Systems. Lancaster University, U.K. http://www.es.lancs.ac.uk.seismicflow/.

Marsh, B.D., 1988. Crystal size distribution (CSD) in rocks and the kinetics and dynamics of crystallization. 1. Theory. Contrib. Mineral. Petrol. 99, 227–291.

Namiki, A., Hatakeyama, T., Toramaru, A., Kurita, K., Sumita, I., 2003. Bubble size distribution in a convecting layer. Geophys. Res. Lett. 30 (15), 1784. doi:10.1029/2003GL017156.

Okumura, S., Nakamura, M., Tsuchiyama, A., Nakano, T., Uesugi, K., 2008. Evolution of bubble microstructure in sheared rhyolite: formation of a channel-like bubble network. J. Geophys. Res. 113, B07208.

Papale, P., 1999. Strain-induced magma fragmentation in explosive eruptions. Nature 397, 425–428.

Phillips, J.C., Lane, S.J., Lejeune, A.M., Hilton, M., 1995. Gum rosin–acetone system as an analogue to the degassing behaviour of hydrated magmas. Bull. Volcanol. 57, 263–268.

Polacci, M., Baker, D.R., Mancini, L., Tromba, G., Zanini, F., 2006. Three-dimensional investigation of volcanic textures by X-ray microtomography and implications for conduit processes. Geophys. Res. Lett. 33, L13312. doi:10.1029/2006GL026241.

Polacci, M., Baker, D.R., Mancini, L., Favretto, S., Hill, R.J., 2009. Vesiculation in magmas from Stromboli and implications for normal Strombolian activity and paroxysmal explosions in basaltic systems. J. Geophys. Res. 114, B01206. doi:10.1029/2008JB005672.

Proussevitch, A.A., Sahagian, D.L., 1998. Dynamics and energetics of bubble growth in magmas: analytical formulation and numerical modeling. J. Geophys. Res. 103, 18,223–18,251.

Proussevitch, A.A., Sahagian, D.L., Tsentalovich, E.P., 2007. Statistical analysis of bubble and crystal size distributions: formulations and procedures. J. Volcanol. Geotherm. Res. 164, 95–111.

Ripepe, M., Marchetti, E., 2002. Array tracking of infrasonic sources at Stromboli volcano. Geophys. Res. Lett. 29. doi:10.1029/2002GL015452.

Ripepe, M., Poggi, P., Braun, T., Gordeev, E., 1996. Infrasonic waves and volcanic tremor at Stromboli. Geophys. Res. Lett. 23, 181–184.

Ripepe, M., Harris, A.J.L., Carniel, R., 2002. Thermal seismic and infrasonic evidences of variable degassing rates at Stromboli volcano. J. Volcanol. Geotherm. Res. 118, 285–297.

Ripepe, M., Marchetti, E., Ulivieri, G., 2007. Infrasonic monitoring at Stromboli volcano during the 2003 effusive eruption: Insights on the explosive and degassing process of an open conduit system. J. Geophys. Res. 112, B09207. doi:10.1029/2006JB004613.

Ripepe, M., Delle Donne, D., Harris, A.J.L., Marchetti, E., Ulivieri, G., 2008. Dynamics of Strombolian Activity. The Stromboli Volcano: An Integrated Study of the 2002–2003 Eruption. Geophysical Monograph Series 182. doi:10.1029/182GM05.

Rust, A.C., Manga, M., 2002. Effects of bubble deformation on the viscosity of diluite suspensions. J. Non-Newtonian Fluid Mech. 104, 53–63.

Sparks, R.S.J., 1978. The dynamics of bubble formation in magmas: a review and analysis. J. Volcanol. Geotherm. Res. 3, 1–37.

Sparks, R.S.J., Brazier, S., 1992. New evidence for degassing processes during explosive eruptions. Nature 295, 218–220.

Stevenson, D.S., Blake, S., 1998. Modelling the dynamics and thermodynamics of volcanic degassing. Bull. Volcanol. 60, 307–317.

Taddeucci, J., Pompilio, M., Scarlato, P., 2004. Conduit processes during the July–August 2001 explosive activity of Mt. Etna (Italy): inferences from glass chemistry and crystal size distribution of ash particles. J. Volcanol. Geotherm. Res. 137, 33–54.

Toramaru, A., 1989. Vesicualtion process and bubble size distribution in ascending magmas with constant velocities. J. Geophys. Res. 94, 17,523–17,542.

Toramaru, A., 1990. Measurements of bubble size distribution in vesiculated rocks with implications for quantitative estimation of eruption processes. J. Volcanol. Geotherm. Res. 43, 71–90.

Turcotte, D.L., 1986. Fractals and fragmentation. J. Geophys. Res. 91, 1921–1926.

Vergniolle, S., Brandeis, G., 1996. Strombolian explosion: 1. A large bubble breaking at the surface of a lava column as a source of sound. J. Geophys. Res. 101 (B09), 20,433–20,448.